

GPO PRICE \$ _____

CFSTI PRICE(S) \$ _____

Hard copy (HC) 3.00

Microfiche (MF) .65

**NASA TECHNICAL
MEMORANDUM**

ff 653 July 65

**NASA TM X-58016
March 1968**



**DEVELOPMENT OF ACOUSTIC TEST CONDITIONS FOR APOLLO
LUNAR MODULE FLIGHT QUALIFICATION**

**By Wade D. Dorland, Robert J. Wren, and Kenneth McK. Eldred
Manned Spacecraft Center
Houston, Texas**

FACILITY FORM 602

<u>N68-21946</u> (ACCESSION NUMBER)	_____ (THRU)
<u>29</u> (PAGES)	<u>1</u> (CODE)
<u>TMX-58016</u> (NASA CR OR TMX OR AD NUMBER)	<u>31</u> (CATEGORY)

NATIONAL AERONAUTICS AND SPACE ADMINISTRATION

ABSTRACT

An acoustic test of an Apollo lunar module was performed prior to flight to verify structural and component integrity. Since the lunar module is enclosed within a spacecraft/lunar-module adapter during the first-stage boost when the dynamic-pressure environment is encountered, the test was performed in accordance with criteria based on measurements of spacecraft/lunar-module-adapter vibration response. The test operations were conducted in the Manned Spacecraft Center Spacecraft Acoustic Laboratory which employs a progressive-wave mode of acoustic excitation and has a duct system tailored to the outer moldline of the Apollo spacecraft. In the lunar-module qualification test, the acoustic spectrum imposed on the spacecraft/lunar-module adapter was nearly as predicted for frequencies above 315 Hz; whereas, the low-frequency spectrum contained more energy than had been predicted. The measured spacecraft/lunar-module adapter responses provided an excellent fit to the flight envelope.

CONTENTS

Section	Page
SUMMARY	1
INTRODUCTION	2
APOLLO VEHICLE AND ENVIRONMENT	3
AVAILABLE DATA AND TEST RATIONALE	4
TEST CONDITIONS	5
FACILITY CALIBRATION PROGRAM	6
VEHICLE TEST PROGRAM	7
Test Sequence	7
Test Results: Acoustic Environment	8
Test Results: Structural Response	8
CONCLUDING REMARKS	9
REFERENCES	10

TABLES

Table	Page
I SPACECRAFT/LUNAR-MODULE ADAPTER FLIGHT MEASUREMENT PARAMETERS	11
II ACOUSTIC TEST SEQUENCE OF LUNAR-MODULE TEST ARTICLE NUMBER 3	12

FIGURES

Figure		Page
1	Lunar module and spacecraft/lunar-module adapter	13
2	Apollo spacecraft and launch vehicles	13
3	Developed view of SLA showing location of skin-panel vibration measurements	14
4	Launch history of SLA vibration during Apollo missions AS-201 and AS-202	15
5	Power spectral density at lift-off (SLA-0)	16
6	Power spectral density at lift-off (SLA-1)	16
7	Power spectral density at lift-off (SLA-2)	17
8	Spectrogram, 1/3-octave band (SLA-0)	17
9	Spectrogram, 1/3-octave band (SLA-1)	18
10	Spectrogram, 1/3-octave band (SLA-2)	18
11	Comparison of predicted Saturn IB and Saturn V lift-off sound-pressure spectra averaged over SLA surface	19
12	Comparison of Saturn IB and smoothed envelope spectra at lift-off over SLA surface	19
13	Vibration envelope adjusted for Saturn V lift-off (SLA-2)	20
14	Arrangement of test vehicle and horn-and-duct system	20
15	Sound-pressure spectra at station X _a 670 in three long-duration LTA-3 tests. The average of 16 ducts in each test and the maximum and minimum values for all three tests are shown	21
16	Average LTA-3 sound-pressure spectra at forward end and aft end of SLA relative to spectra at the mid-SLA location	21
17	Sound-pressure spectra measured inside the SLA (and external to LTA-3) and inside the LTA-3 ascent-stage crew compartment	22
18	Noise reduction through SLA and LTA-3	22

Figure		Page
19	Comparison of LTA-3 test and predicted spectra on SLA exterior	23
20	Response spectrogram (SLA-0)	23
21	Response spectrogram (SLA-1)	24
22	Response spectrogram (SLA-2)	24

**DEVELOPMENT OF ACOUSTIC TEST CONDITIONS FOR APOLLO
LUNAR MODULE FLIGHT QUALIFICATION**

By Wade D. Dorland, Robert J. Wren, and Kenneth McK. Eldred*
Manned Spacecraft Center

SUMMARY

As part of a comprehensive ground-test program to verify structural and component integrity prior to flight, an Apollo lunar module was subjected to an acoustic test which simulated realistically the dynamic-pressure environment encountered during launch of the Apollo spacecraft. Inasmuch as the lunar module is enclosed within a spacecraft/lunar-module adapter during the first-stage boost when the dynamic-pressure environment is encountered, the test conditions were based upon measurements of adapter vibration response obtained from two early unmanned Apollo missions. The data included the following three characteristic periods of interest: (1) lift-off noise, (2) transonic aerodynamic excitation, and (3) supersonic aerodynamic excitation. An adapter response condition which enveloped these data was established for the test.

The test operations were conducted in the Manned Spacecraft Center Spacecraft Acoustic Laboratory which employs a progressive-wave mode of acoustic excitation and a duct system which is tailored to the outer moldline of the Apollo spacecraft. Prior to performing the lunar-module test calibration, test runs were conducted using an assembly of Apollo modules without the lunar module. The spacecraft assembly, which represented the unmanned flight configuration, was then excited acoustically, and the conditions of acoustic excitation were varied until the required adapter response was obtained. The lunar module then was inserted in the test assembly, and the qualification test was performed.

The resulting acoustic spectrum imposed on the adapter was very similar to the predicted spectrum above 315 Hz; however, the low-frequency test spectrum contained more energy than had been predicted. The measured response of the adapter to the test excitation provided an excellent fit to the flight envelope.

*Director of Research, Wyle Laboratories, El Segundo, California.

INTRODUCTION

Verification of the capability of the Apollo lunar module (LM) to sustain the dynamic loads experienced during launch necessitated the performance, prior to the launching of the first LM vehicle, of a comprehensive ground-test program to qualify the structure and system components for flight. As a part of this ground-test program, an acoustic test was performed to simulate realistically the dynamic-pressure¹ environment which exists during the launch-and-boost phase of an Apollo mission. Since the LM acoustic testing imposed certain uncommon environmental-simulation requirements, the resulting test operation incorporated several newly devised experimental techniques which are considered to be an important contribution to acoustic testing technology.

Throughout the launch-and-boost phase, the LM is located within the spacecraft/LM adapter (SLA). The LM is attached at four points to the SLA which is a truncated cone 28 feet long that fairings the spacecraft into the Saturn IVB (S-IVB) stage (fig. 1). During the initial phase of flight, the dynamic environment exterior to the vehicle has three distinct characteristics of interest.

1. Booster noise at lift-off, a zero-velocity condition
2. Aerodynamic excitation in the transonic-velocity condition
3. Aerodynamic excitation in the supersonic-velocity condition

The environment inside the SLA, however, is a function of the dynamic energy transmitted through the structure; hence, the interior environment is largely determined by the SLA response to exterior excitation. This aspect of the LM environment introduces an unusual consideration into the determination of adequate ground-test conditions, since current analytical techniques do not yield precise environmental definitions for a test article that is mounted inside an adapter. Accordingly, an experimental procedure was needed which obviated the requirement for analytically derived test environments. Such a procedure was devised for this project. The procedure was based on the rationale that the environment for the LM is a combined result of the acoustic field in the SLA and the vibration transmitted through the SLA attachment fittings. The LM environment is uniquely related to the SLA dynamic response; therefore, the proper LM environment could be obtained in the laboratory only by exciting the SLA to flight response. To support such an experimental procedure, data which were recorded from three flight pickups during each of the first two Apollo missions were used to define the required SLA vibration response. Application of this procedure enabled the adjustment of the laboratory acoustic spectrum to compensate for the difference in the spatial distribution of phase-correlation coefficients which exist in flight and laboratory environments. Therefore, the acoustic field was

¹The expression "dynamic pressure" will refer to the acoustic and high-frequency, unsteady fluctuating-pressure components of the total pressure environment. "High frequency" in this context refers to that part of the audio spectrum between 20 and 2500 Hz.

controlled for the specified SLA vibration response rather than for faithful simulation of a predicted flight fluctuating-pressure environment. It is significant that the acoustic spectrum actually imposed on the SLA in the laboratory contained more low-frequency energy than was predicted for the lift-off environment; whereas, the high-frequency spectrum (above 315 Hz) was nearly as predicted. The increased low-frequency energy was not undesirable but illustrates how the empirically determined test conditions differed from predicted conditions.

The acoustic testing of the LM was performed in the Manned Spacecraft Center Spacecraft Acoustic Laboratory (MSC SAL). This facility employs a progressive-wave mode of acoustic excitation and has a duct system which is tailored to the outer moldline of the Apollo spacecraft. The ducts, in combination with controllable acoustic noise generators, provide the capability to control the acoustic energy levels, the spectral distribution (in 1/3-octave bands), the longitudinal dynamic-pressure profile, the circumferential dynamic-pressure profile, and the approximate circumferential space correlation of the acoustic field. Prior to the LM acoustic test, a sequence of test runs was performed on an Apollo spacecraft. During these test runs, the acoustic field was tailored to produce an SLA response that simulated flight response.

In the following sections of this report, the simulation problem will be described. This description will include the vehicle and the launch environment. The next section will include the available environmental and response data, the test rationale, and the derivation of the test criteria. After a brief description of the test facility, the experimental program used to prepare the facility for the LM acoustic test will be presented. In addition, the test results will be presented.

APOLLO VEHICLE AND ENVIRONMENT

The Apollo spacecraft launch configuration embodies a complex of various spacecraft and launch-vehicle modules. The spacecraft launch configuration, based on specific mission objectives, may consist of a launch escape system (LES), the command and service modules (CSM), the LM, an SLA, an SLA nose cone, and the launch vehicle (which is a Saturn booster configuration). Two configurations of particular interest for ground-test simulation are: a spacecraft configuration of an LES, the CSM, and an SLA which would be launched by an uprated Saturn I booster (S-IB and S-IVB stages) or this spacecraft configuration with an LM added which would be launched by the Saturn V booster (S-IC, S-II, and S-IVB stages). Also of interest is a mission involving an LM mounted inside an SLA, with a nose cone attached to the forward end of the SLA. This spacecraft configuration would be launched by an uprated Saturn I booster. In all missions, the instrument unit (IU) provides the mechanical interface between the spacecraft and the launch vehicle. The external dimensions (or moldline) of the CSM, the SLA, and the IU remain constant. Figures 1 and 2 show the arrangement of the modules at launch.

Since, as previously mentioned, the structural response of the SLA is a key factor in the LM acoustic test, the SLA structure must be described in some detail. The SLA is a truncated cone comprised of eight panels. Four of the panels, such as the forward section, have linear explosive charges installed at panel junctions. During

CSM/SLA separation, the charges are fired to open the four panels, which frees the CSM from the launch vehicle and exposes the LM (fig. 1). The other four panels make up an integrated aft section which remains attached to the IU throughout the flight. The SLA diameter is 155 inches at the SM interface and 260 inches at the IU interface. The adapter is 336 inches high and has a slant height of 349 inches and a slant angle of 8.6° . Each of the eight panels is constructed of several aluminum-honeycomb subpanels, and the eight panels are joined by stiffeners that have the same radial thickness as the honeycomb face sheets. Thus, in appearance, the composite of subpanels and stiffeners forms a smooth curved surface for one panel. The structural dynamic properties of the panels are controlled essentially by the honeycomb subpanels and not by the stiffeners, so that each panel behaves as a continuous, curved honeycomb shell segment. The panels are joined by bolted doubler plates on internal and external surfaces. At the LM attachment station (81 inches forward of the SLA/IU interface), a light ring stiffener is employed at the joint between the forward and aft sections. The entire SLA can be considered to be a continuous, uniform shell composed only of the honeycomb structure used in the construction of the subpanels. This honeycomb is constructed of Type 2024T-81 aluminum alloy that is 1.7 inches thick and has a surface weight density of approximately 2 lb/ft^2 . The entire SLA assembly weighs approximately 3600 pounds. During unmanned CSM flights, the LM is replaced in the SLA by the flight stabilizer which is a simple crossed truss weighing approximately 60 pounds. During missions which require the LM, the SLA supports the full weight of the CSM (approximately 70 000 pounds) and of the LM (approximately 30 000 pounds).

At lift-off, during the launch-and-boost phase, the Apollo spacecraft is exposed to an acoustic environment that is generated by the exhaust turbulence of the first-stage booster engines. Additional dynamic-pressure environments envelop the spacecraft during the transonic and supersonic portions of flight, but no significant pressure environments excite the spacecraft at velocities in excess of Mach 3. In all these conditions of first-stage boost, the spacecraft/launch-vehicle configuration is the same. Accordingly, a single test-article setup is sufficient for a ground-test simulation of the launch dynamic environment.

AVAILABLE DATA AND TEST RATIONALE

In the development of the Apollo spacecraft, nearly all of the early effort for environmental definition was concentrated on the CSM, and only the forward section of the SLA was included in this work. After most of the early definition had been accomplished, the shape of the SLA was drastically altered, thus nullifying the validity of this early effort (both analytical and experimental) as applied to the SLA or the LM. The LM vehicle designers had employed a comparability technique based on Barrett's method (refs. 1 and 2) to establish early LM environmental descriptions. It was recognized that the LM environment was a combined result of the acoustic field in the SLA and of the vibration transmitted through the SLA attachment fittings on the descent-stage outriggers. Barrett's method is an accepted procedure for deriving launch-vehicle structural test requirements. However, application of this technique to LM environment definition presented difficulties since Barrett's method is based on the assumption that similar structural configurations exhibit similar dynamic characteristics. The difference between the environmental excitation of the Saturn launch

vehicle and LM structures contributes a significant uncertainty to the application of Barrett's method. Hence, the anticipated noise reduction of the SLA was calculated, and the resulting lower LM vibration levels were used as structural and equipment specifications for design and qualification purposes. By using this modification of Barrett's method, overly conservative vibration levels were avoided. One important test objective, therefore, was the verification of the predicted SLA noise reduction and of the resulting LM vibration.

To achieve this objective, a test procedure was devised that used the limited flight data which were available on the response of the SLA panels to obtain the required test conditions. In this procedure, the proper LM environment could be obtained in the laboratory by exciting the SLA so that the SLA response matched the flight data as nearly as possible. The motion of the SLA panels in response to external environmental excitation serves as a source of excitation of the internal SLA airmass; therefore, the acoustic field inside the SLA during a test closely simulates the internal SLA acoustic field experienced during flight, if the response is the same in both the test and the flight. Hence, this excitation of the LM is realistic. Also, the LM receives a small amount of dynamic excitation through the LM attachment points to the SLA. Since the test configuration of the SLA and the SLA/LM mating components in the laboratory closely duplicates the SLA flight configuration (with only minor exceptions), the LM excitation through the attachment points is essentially the same in both situations. Accordingly, the total dynamic excitation of the LM acoustic test closely simulates flight conditions.

TEST CONDITIONS

As mentioned previously, limited SLA vibration measurements were obtained during early Apollo spacecraft missions. The measurements, which were made at three asymmetric points, indicated motion in the radial direction. (The locations of the points are shown in the sketch of the SLA in fig. 3. The measurements are designated SLA-0, SLA-1, and SLA-2.) Identical measurements were made on two flights which followed very similar boost profiles. The records of overall root-mean-square vibration level g_{rms} as a function of range time for all six measurements (i. e., records for each of three locations during each of two flights) are shown in figure 4, and a tabulation of measurement parameters is given in table I. Inspection of these data shows that the characteristics with time of the two flights are very similar. In addition, the conditions of maximum response (i. e., lift-off, transonic velocity, and supersonic velocity) are clearly evident. Plots of acceleration power spectral density (PSD) for the response at lift-off are presented in figures 5 to 7, and 1/3-octave-band spectrograms for all three response conditions are plotted in figures 8 to 10. Again, from the spectral plots, a rather remarkable repeatability of the vibration is evidenced in the two flights.

Since the electronic control system of the MSC SAL (ref. 3) provides spectral control in 1/3-octave bandwidths, test conditions were developed using corresponding bands. Only one spectral condition could be programed in the test; therefore, it was necessary to reduce the number of applicable spectra to a single spectrum at each location. Examination of the spectra for the different flight times at each

measurement location (figs. 8 to 10) revealed that the range of spectral levels in each band was nominally 15 dB or a half order of magnitude. Furthermore, the lift-off spectrum was observed to dominate, except for the very low and the very high frequencies where the transonic response is higher. (As a peripheral observation, supersonic response does not dominate any portion of the spectrum at any of the three locations.) Enveloping the spectral data points would produce slightly more strenuous test conditions than would averaging the data, but in a flight simulation, such an envelope spectrum for each location is advantageous in obtaining a reasonable, but not prohibitive, degree of conservatism in the test. Also, an envelope spectrum is not likely to result in an undertest and, thus, preclude satisfying the test requirements. Accordingly, a spectrum envelope was drawn for each location to the highest values of figures 8 to 10 as the initial determination of the test conditions.

The domination of the resulting spectral envelope by lift-off conditions required another consideration to be included in the test conditions. That is, although the LM would be launched by both the Saturn IB and the Saturn V vehicles, the foregoing test conditions included only environmental characteristics of the Saturn IB launches. During lift-off, however, the Saturn V booster noise would impose higher sound-pressure levels (SPL) below 100 Hz on the SLA surface, as indicated in figure 11. Consequently, test conditions derived from Saturn IB flight measurements would be insufficient to insure that the LM would adequately survive the Saturn V lift-off environment. To overcome this problem, the envelope spectra were adjusted for the difference in lift-off environments.

Consideration also was given to increased transonic and supersonic excitation caused by higher aerodynamic pressures in Saturn V boost, as compared to Saturn I boost. Nominally, the measured response of the SLA would be increased by 2 dB to account for this change. However, since transonic excitation of the SLA is higher than lift-off excitation only in the extreme limits of the measured spectrum, this adjustment would have negligible effect on the overall excitation levels or response characteristics. Accordingly, no adjustment was needed in the test conditions for differences in the Saturn I and Saturn V transonic-dynamic pressures.

A smoothed envelope of the environment spectra from figure 11 and the Saturn IB environment spectrum are both plotted in figure 12. The difference in these spectra was applied (added arithmetically) to the SLA response spectra. For example, the SLA-2 response envelope, shown by the solid curve in figure 13, was adjusted between 40 Hz (the lowest frequency of lift-off dominance) and 125 Hz (the highest frequency of lift-off spectral difference). The revised portion of the spectrum is indicated by the dashed curve. The resulting test spectrum for SLA-2 is shown in figure 13 by the dashed curve between 40 and 100 Hz and by the solid curve at all other frequencies. Similar adjustments also were made on the SLA-1 and SLA-0 measurements, thus yielding the three response-control spectra for the LM acoustic test.

FACILITY CALIBRATION PROGRAM

The MSC SAL, which was designed and equipped to perform environmental tests of full-scale manned spacecraft, is described in detail in reference 3. In the LM

project, the CSM and the SLA were surrounded by an assembly of 16 ducts through which plane-wave acoustic energy was propagated. Each duct in this arrangement (designated the horn-and-duct system) was driven by an independent air-modulator noise source, as shown in figure 14. Thus, an annular sound field was formed which was divided into 22.5° segments. Sound levels in the longitudinal direction can be controlled by moving the outer wall of the ducts in and out radially which varies the duct-to-test-vehicle clearance. Each air modulator is controlled by an independent channel of the SAL electronic control system where such a channel provides control of overall level, of spectrum shape in 1/3-octave bands, and of limited phase correlation between channels. Hence, the sound field can be optimized in each duct for level and spectrum, and circumferential correlation around the vehicle (i. e., between ducts) can be controlled to a limited extent. The spectrum in each duct is shaped by a 1/3-octave-band shaper, but control is exercised by using a microphone to measure the sound field in the duct at a selected point. The shaper controls were manipulated until the required spectrum was measured. However, control below 50 Hz is limited by the rolloff characteristics of the coupling horn between the air modulator and the duct. Also, above 315 Hz, control is limited by the fact that much of the sound energy in a duct is generated by harmonic distortion of the lower frequency energy. The total weight of the horn-and-shroud system is supported by the SAL tower structure so that this assembly adds no load to the test vehicle. A soft, uninflated hose is used to seal each radial duct wall to the test-vehicle surface. Minimal restraint is exerted by these seals on the displacement of the vehicle skin.

Although the MSC SAL has the capability to adjust and control the spatial-correlation characteristics of the acoustic field, the best fit to the desired SLA response is obtained with a control mode in which each air modulator is controlled by a separate electronic noise generator. Previous experiments (ref. 3) have shown that the facility has more than sufficient capability to drive the SLA to the required response levels. In other tests in the MSC SAL, the SLA has produced a very uniform response at all points on its surface; thus, it was concluded that laboratory fixtures were not introducing any undesirable anomalies into the SLA response. Furthermore, the specific SLA being used in the laboratory has been shown to behave in accordance with the salient features of a monocoque, continuous truncated cone when excited by a dynamic forcing function (ref. 4).

Starting with arbitrary test conditions, the LM calibration runs were arranged to vary acoustic-field parameters until a best-fit SLA response was obtained and until the sound fields within the various ducts had reasonably small variations. (At the conclusion of these calibration runs, the ducts were disassembled, and the SLA forward and aft sections were separated in preparation for installing the LM test article.)

VEHICLE TEST PROGRAM

Test Sequence

After the LM test article was mated to the SLA and the horn-and-duct system was assembled around the vehicle, a sequence of eight acoustic tests was performed. This sequence is tabulated in table II. The specific test article used for this program

was LM test article number 3 (LTA-3). This was a complete structural demonstrator with an unabridged complement of prototype or mass-representative equipment and subsystems. Consequently, this sequence of tests was designated the LTA-3 acoustic test.

Test Results: Acoustic Environment

The acoustic field imposed on the SLA exterior is shown in figure 15. The average spectrum for each of the three long tests (35 seconds or more) is shown, and the envelopes show the maximum and minimum values measured in each 1/3-octave band in any duct during the three tests. Repeatability of the levels from test to test was very good. This spectrum was measured at station X_a 670 which is midway along the length of the SLA. The spectral consistency along the length of the SLA is indicated in figure 16. The average SPL spectrum is plotted at station X_a 778 (near the forward end of the SLA) relative to station X_a 670 and at station X_a 552 (near the aft end of the SLA) relative to station X_a 670. If the field were the same at all three locations, both curves would converge to 0 dB. The major deviation is in the low-frequency bands near the cut-off frequency of the horn. However, this deviation is not considered to be serious since the SLA has relatively low excitation and acceptance. The SPL in the 31-Hz bandwidth is 7 dB below the bandwidth of highest SPL (at 100 Hz), and the typical SLA response (in the 31-Hz bandwidth) is 22 dB below the bandwidth of maximum response (at 250 Hz). Except for an undesirable peak at 400 Hz, the deviation is an average of 3 dB or less between 50 and 1000 Hz.

The acoustic field inside the SLA (but external to the LM) was measured with 18 microphones placed around the LM in a configuration that was a rough approximation of a sphere. The results of these measurements and the sound spectrum measured inside the LM ascent-stage crew compartment with a single microphone are shown in figure 17. (Data from this microphone are not entirely applicable for extrapolating flight conditions since LTA-3 lacked certain interior furnishings which will be installed on flight articles; in addition, the LTA-3 cabin walls had several open penetrations which will be sealed in the flight articles.) Figure 18 is a plot of the SLA noise reduction (i. e., the average SLA external spectrum minus the SLA average internal spectrum) and of the LM noise reduction (i. e., the SLA average internal spectrum minus the LM internal spectrum). Finally, figure 19 is a plot of the SLA external spectrum, a predicted S-IB lift-off spectrum on the SLA exterior, and an SLA external transonic spectrum, as contained in the Apollo certification test requirement (CTR). The comparison with the transonic spectrum is of interest since this predicted spectrum had been used to derive vibration specifications for the qualification of LM components and equipment (ref. 5).

Test Results: Structural Response

The response spectra for locations SLA-0, SLA-1, and SLA-2 are presented in figures 20, 21, and 22, respectively. In each figure, curves indicating the response during the calibration run (identified as "empty SLA") and the LTA-3 test are plotted with the flight envelope or response-control spectrum. The SLA responses at

locations SLA-1 and SLA-2 during the calibration test provided an excellent fit to the flight envelope, but the response of SLA-0 generally exceeded the flight envelope. However, the flight response of SLA-0 was not consistent with the flight responses of SLA-1 and SLA-2. This inconsistency may be artificial in that the telemetry bandwidth of SLA-0 was narrower than for either SLA-1 or SLA-2; consequently, the negative slope above 160 Hz is attributed to the limited response of the measurement equipment used in flight. If the response up to 160 Hz were extrapolated with a response characteristic, as shown in the other two measurements, a peak could be expected at 250 Hz of approximately the same amplitude as the laboratory-induced response. On this basis, the slightly poorer fit of laboratory-induced response to flight response is acceptable.

The response of the SLA during the LTA-3 test was lower in the frequency range from 80 to 800 Hz at locations SLA-1 and SLA-2 than was measured in the calibration test in which the SLA was empty. The aft-section response (as indicated by SLA-0) was almost identical for the calibration and LTA-3 tests. The small changes in response could be attributed to the effect on the SLA structural dynamics of supporting an additional 30 000 pounds, or the internal sound levels could be lower as a result of the absorption of acoustic energy by the LM. Since SLA internal sound pressures were not measured during the calibration test (empty SLA), the absorption of the LM is not known. In any case, an explanation of the causes of the SLA response variations is not forthcoming from the data obtained in this program.

CONCLUDING REMARKS

Flight certification of the lunar module required an acoustic test to verify the structural integrity of the lunar module to the high-frequency dynamic-pressure environment encountered in launch and to define or to verify equipment-qualification vibration-test requirements. This test was performed using a structural demonstrator vehicle which was designated lunar-module test article number 3. The test environment was evolved from a facility calibration program which culminated in a preparatory run and which produced the best possible match of laboratory response to launch response in the empty spacecraft/lunar-module adapter. The spacecraft/lunar-module adapter response was a key factor in obtaining a faithful simulation of the flight environment since the spacecraft/lunar-module adapter shrouds the lunar module during the portion of launch when the dynamic-pressure environment exists. The lunar-module environment is, therefore, a unique function of the spacecraft/lunar-module adapter response. Knowledge of the spacecraft/lunar-module adapter response has been obtained at three locations during the launch of Apollo-Saturn 201 and Apollo-Saturn 202. Enveloping the maximum spectral values obtained from these flights produced the spectrum used for the test requirements. Close adherence to this spectrum was obtained in both the calibration and in the tests of lunar-module test article number 3, indicating a highly realistic test of the lunar module in the flight environment.

In the testing of the lunar module, the high degree of similarity between the spacecraft/lunar-module structural-vibration responses measured in the acoustic laboratory and the responses measured in flight demonstrates that successful

simulation of environmental excitation can be obtained without complete definition of the environmental criteria. Such a demonstration marks a step forward in the application of ground-test facilities in achieving more realistic flight simulations.

Manned Spacecraft Center
National Aeronautics and Space Administration
Houston, Texas, March 29, 1968
914-50-20-15-72

REFERENCES

1. Barrett, R. E.: Techniques for Predicting Localized Vibratory Environments of Rocket Vehicles. NASA TN D-1836, 1963.
2. Barrett, R. E.: Statistical Techniques for Describing Localized Vibratory Environments of Rocket Vehicles. NASA TN D-2158, 1964.
3. Wren, R. J.; Dorland, W. D.; and Eldred, K. McK.: Concept, Design, and Performance of the Spacecraft Acoustic Laboratory. Bulletin of the 37th Shock and Vibration Symposium, Orlando, Fla., Oct. 24-26, 1967.
4. White, R. W.: Predicted Vibration Responses of Apollo Structure and Effects of Pressure Correlation Lengths on Response. Wyle Laboratories Rept. WR 67-4, El Segundo, Calif., Mar. 1967.
5. Anon.: The LTA-3 Ascent Stage and Descent Stage Thermal Shielding and Support Structure. Lunar Module Certification Test Requirement no. LCQ-560-373, July 14, 1966.

**TABLE I. - SPACECRAFT/LUNAR-MODULE ADAPTER
FLIGHT MEASUREMENT PARAMETERS**

Parameter	Mission	
	AS-201	AS-202
Flight parameter time, sec		
Engine ignition	-1.7	-1.2
Lift-off	.37	.93
Mach 1	65	64
Max Q	75	79.0
Mach 2	89	87
Data reduction slice time, sec		
Lift-off	-1.0 to 1.0	-1.0 to 2.0
Transonic	61.5 to 63.5	59.5 to 62.5
Supersonic	88.0 to 90.0	84.0 to 87.0
Max Q peak value, lb/ft²	625	665
Nominal data bandwidth, Hz		
SLA-0	5 to 220	5 to 220
SLA-1	5 to 330	5 to 330
SLA-2	5 to 450	5 to 450

**TABLE II. - ACOUSTIC TEST SEQUENCE OF LUNAR-MODULE
TEST ARTICLE NUMBER 3**

Level			Duration		Remarks
Test no.	High or low	SPL, dB	Long or short	Time, sec	
1	Low	139	Long	65	Facility checkout run
2	High	152	Short	18	Establish data acquisition system gain settings
3	High	152	Long	42	Data acquisition with channels 1 to 275
4	High	152	Short	19	Establish data acquisition system gain settings
5	High	152	Long	38	Data acquisition with channels 276 to 550
6	High	152	--	5	Prematurely terminated by equipment malfunction
7	High	152	Short	18	Establish data acquisition system gain settings
8	High	152	Long	41	Data acquisition with all channels missed on previous runs

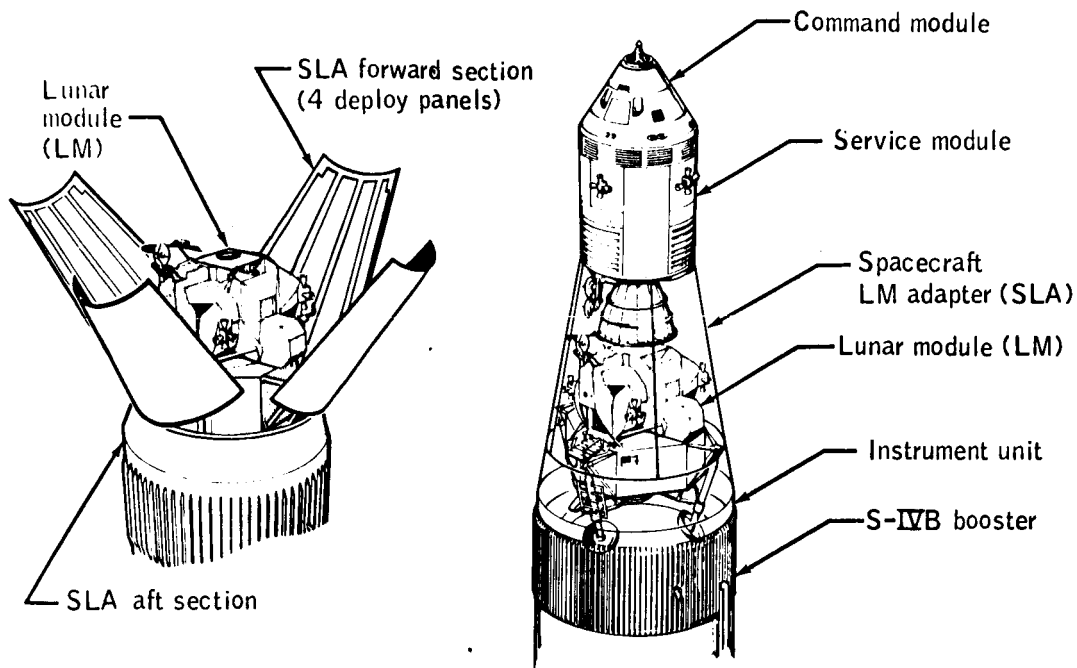


Figure 1. - Lunar module and spacecraft/lunar-module adapter.

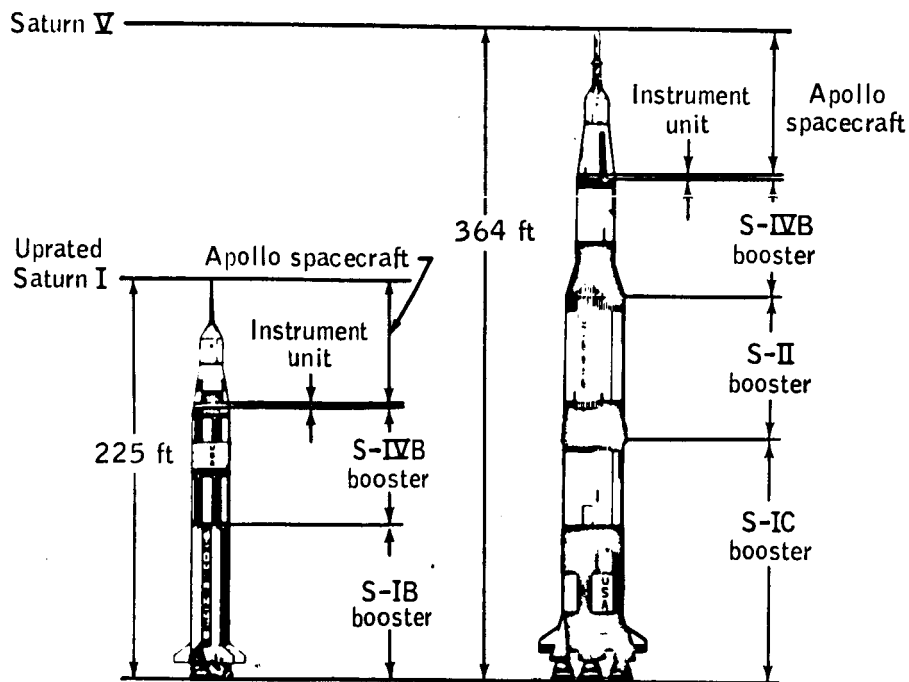


Figure 2. - Apollo spacecraft and launch vehicles.

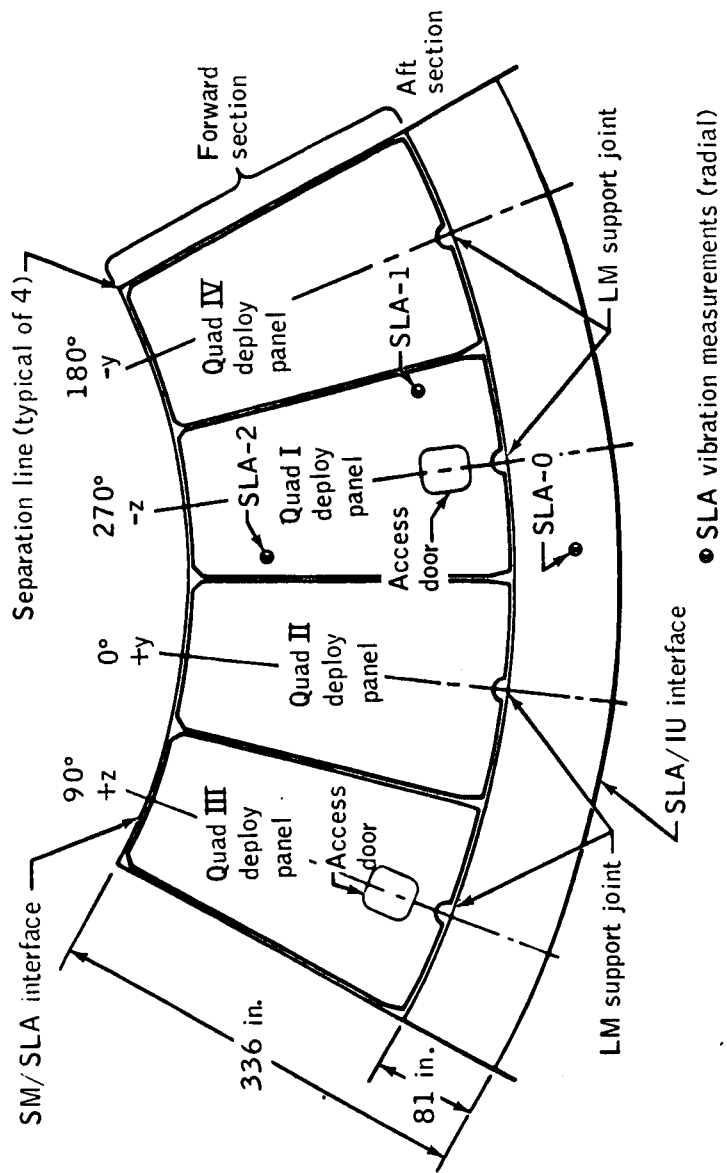


Figure 3. - Developed view of SLA showing location of skin-panel vibration measurements.

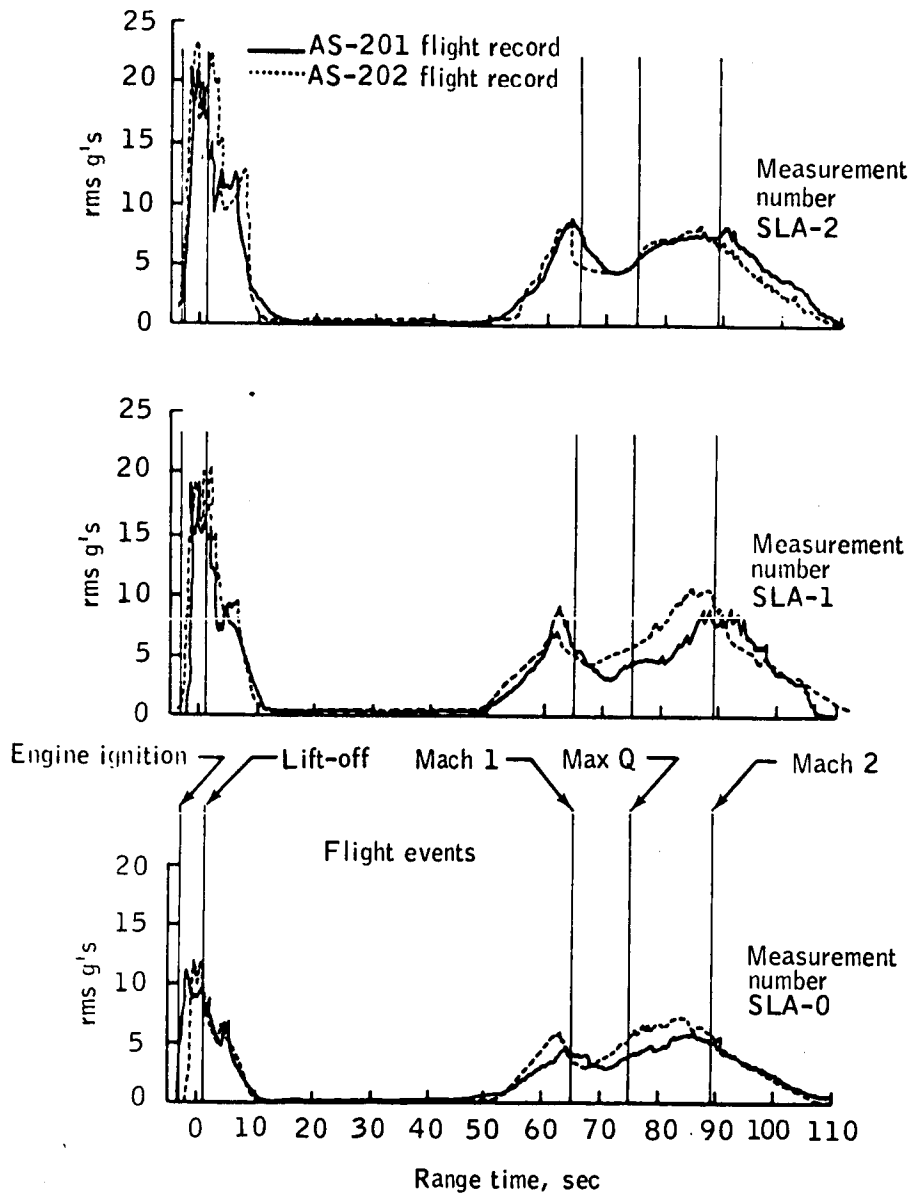


Figure 4. - Launch history of SLA vibration during Apollo missions AS-201 and AS-202.

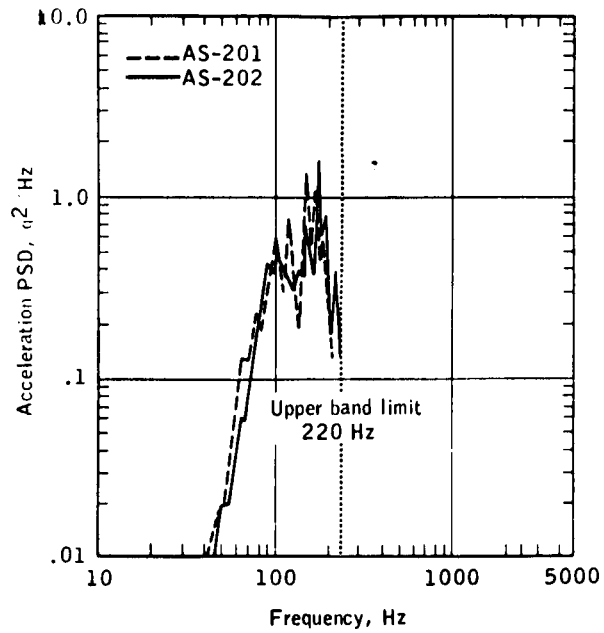


Figure 5. - Power spectral density at lift-off (SLA-0).

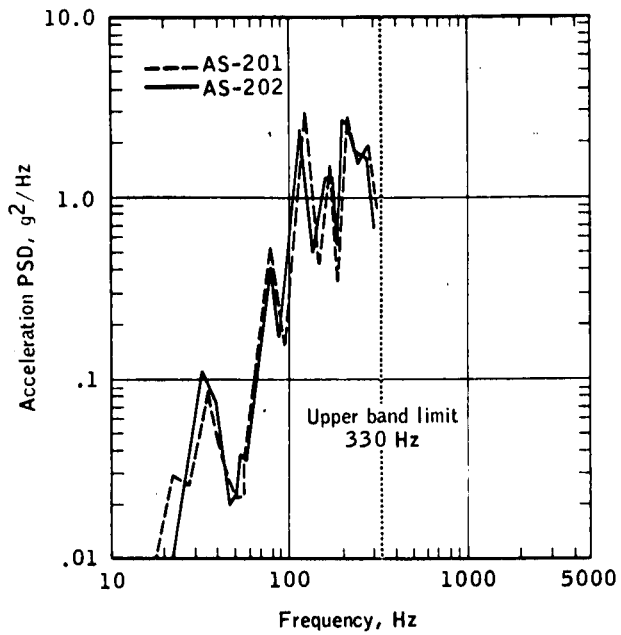


Figure 6. - Power spectral density at lift-off (SLA-1).

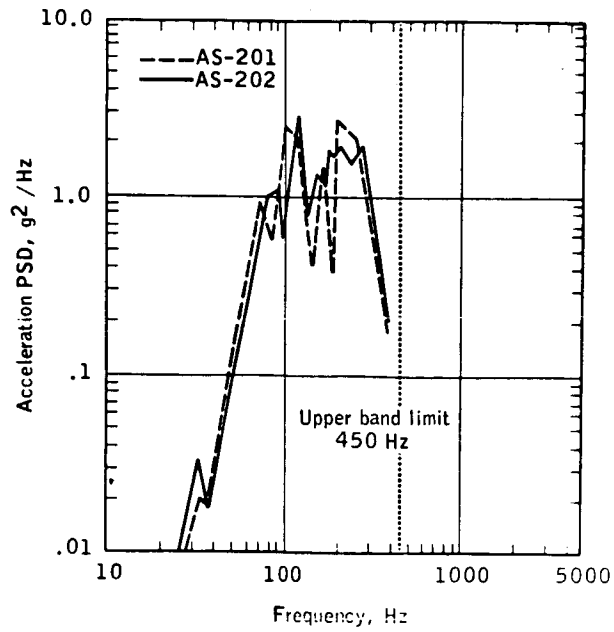


Figure 7. - Power spectral density at lift-off (SLA-2).

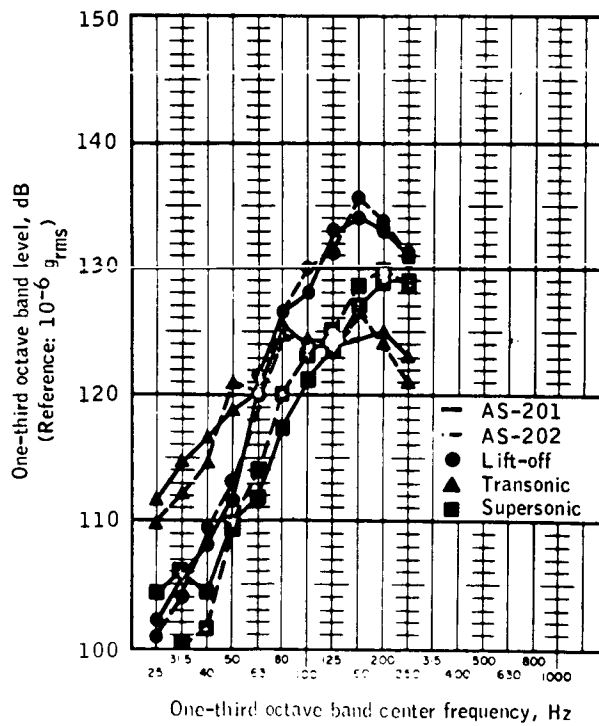


Figure 8. - Spectrogram, 1/3-octave band (SLA-0).

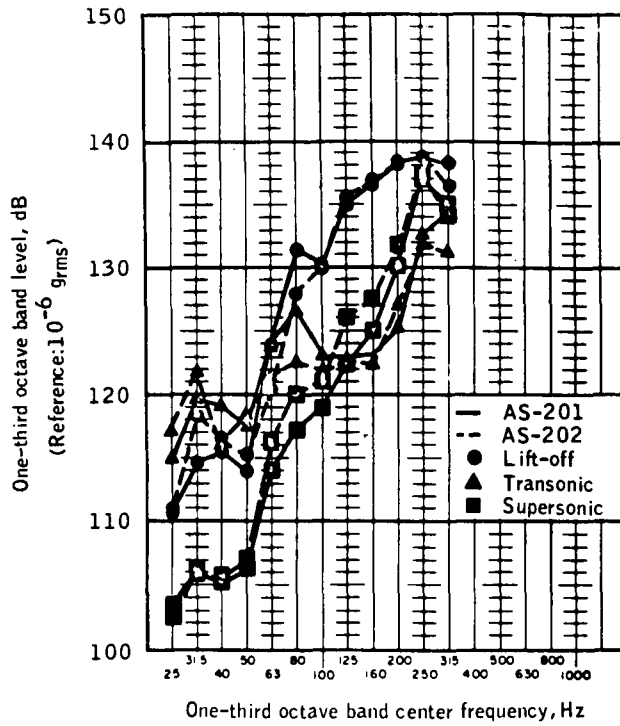


Figure 9. - Spectrogram, 1/3-octave band (SLA-1).

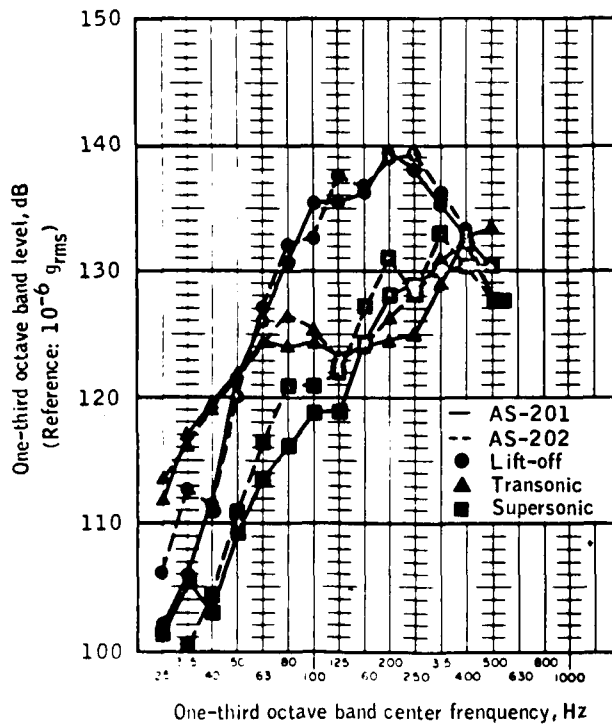


Figure 10. - Spectrogram, 1/3-octave band (SLA-2).

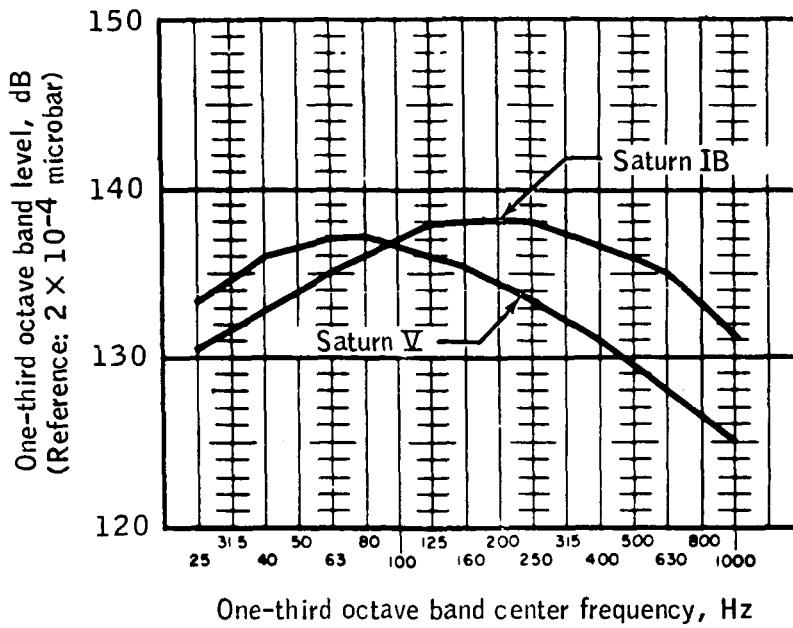


Figure 11. - Comparison of predicted Saturn IB and Saturn V lift-off sound-pressure spectra averaged over SLA surface.

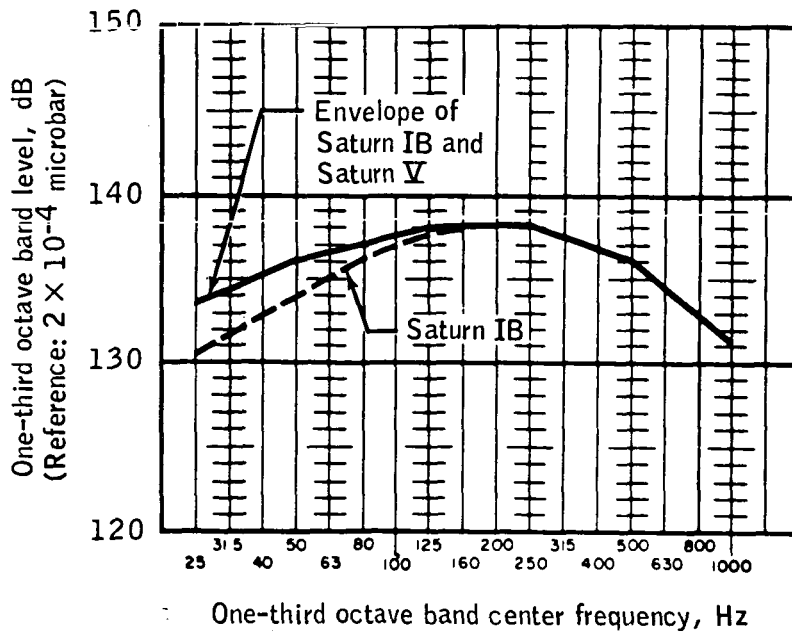


Figure 12. - Comparison of Saturn IB and smoothed envelope spectra at lift-off over SLA surface.

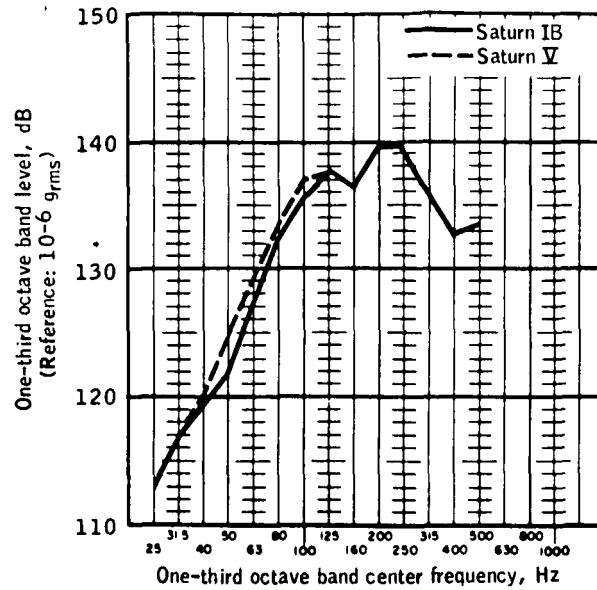


Figure 13. - Vibration envelope adjusted for Saturn V lift-off (SLA-2).

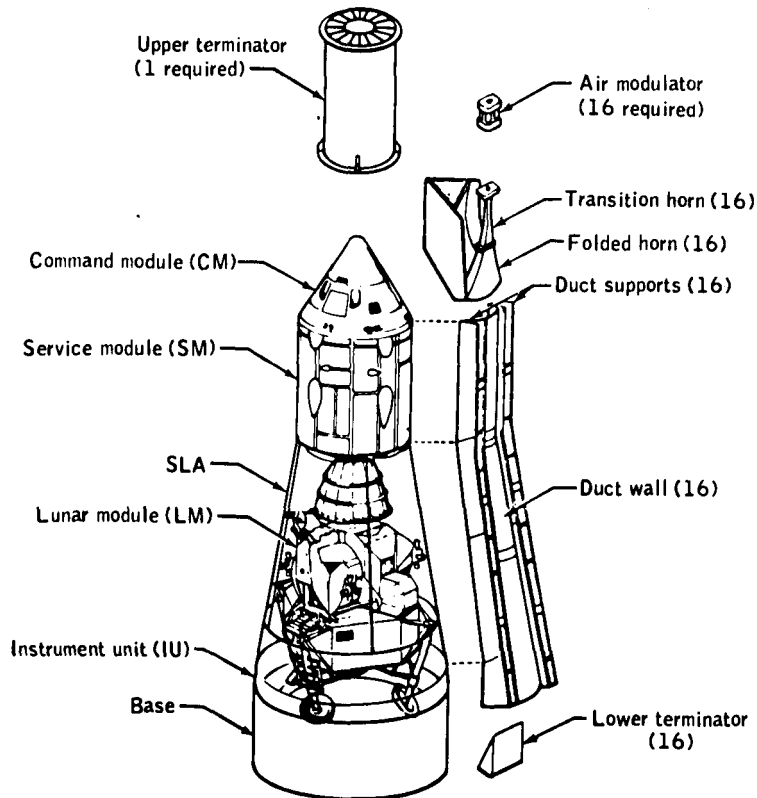


Figure 14. - Arrangement of test vehicle and horn-and-duct system.

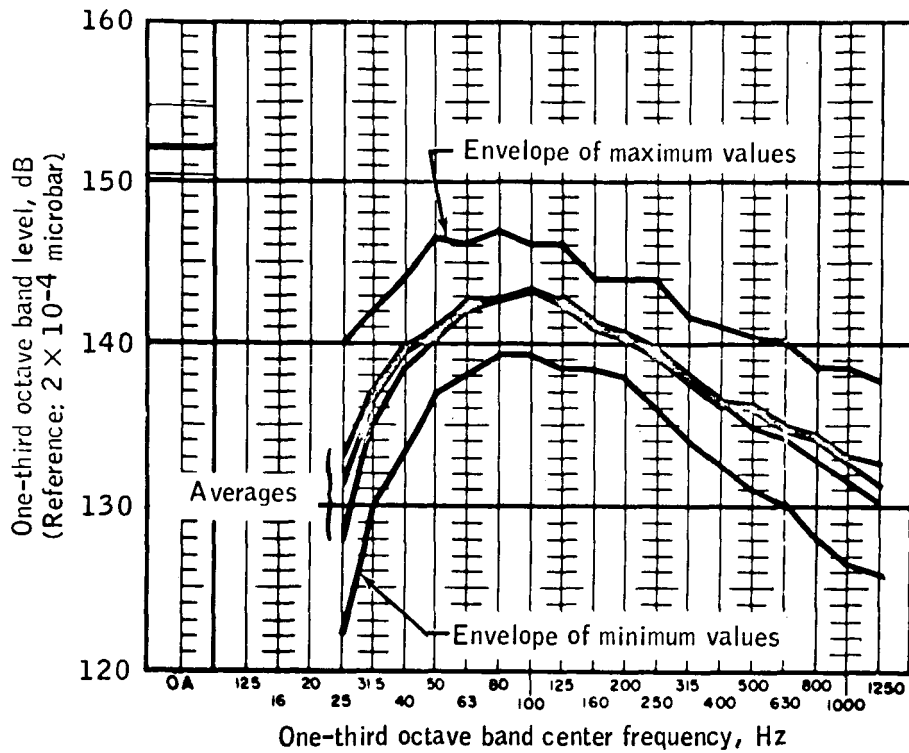


Figure 15. - Sound-pressure spectra at station X_a 670 in three long-duration LTA-3 tests. The average of 16 ducts in each test and the maximum and minimum values for all three tests are shown.

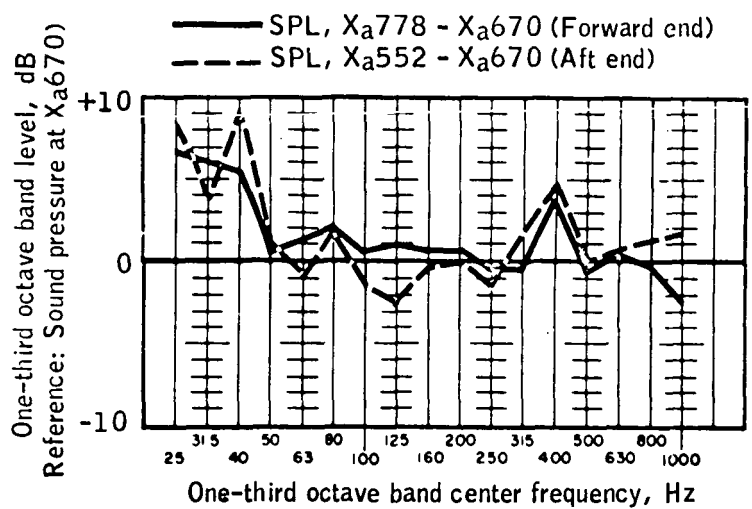


Figure 16. - Average LTA-3 sound-pressure spectra at forward end and aft end of SLA relative to spectra at the mid-SLA location.

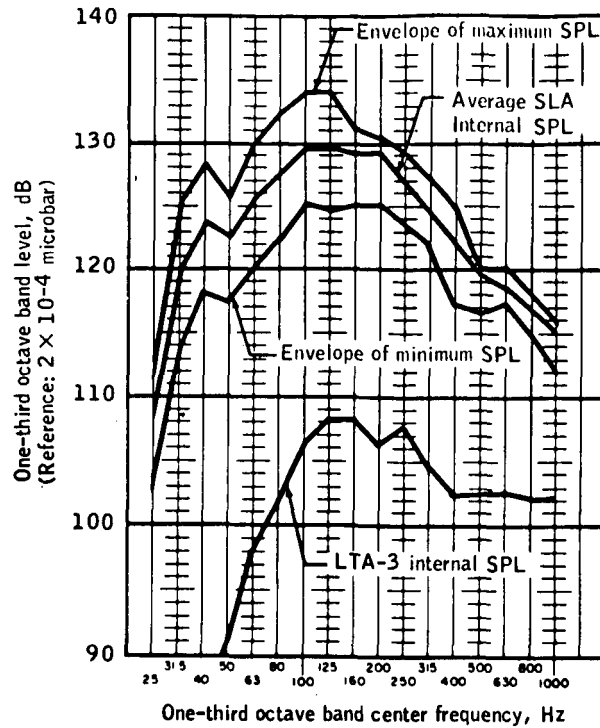


Figure 17. - Sound-pressure spectra measured inside the SLA (and external to LTA-3) and inside the LTA-3 ascent-stage crew compartment.

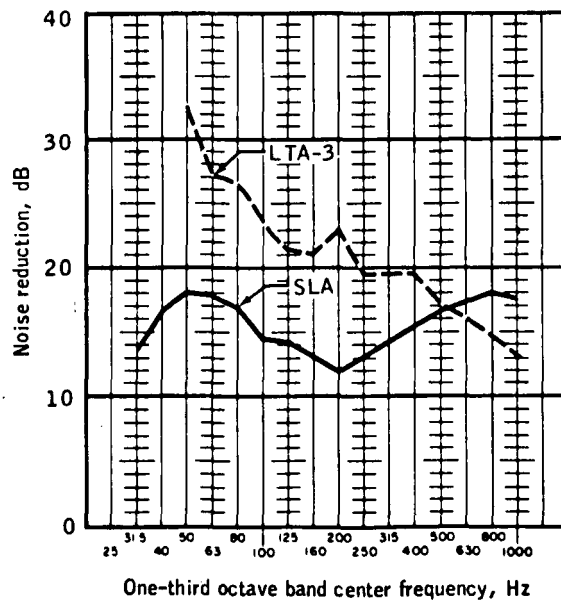


Figure 18. - Noise reduction through SLA and LTA-3.

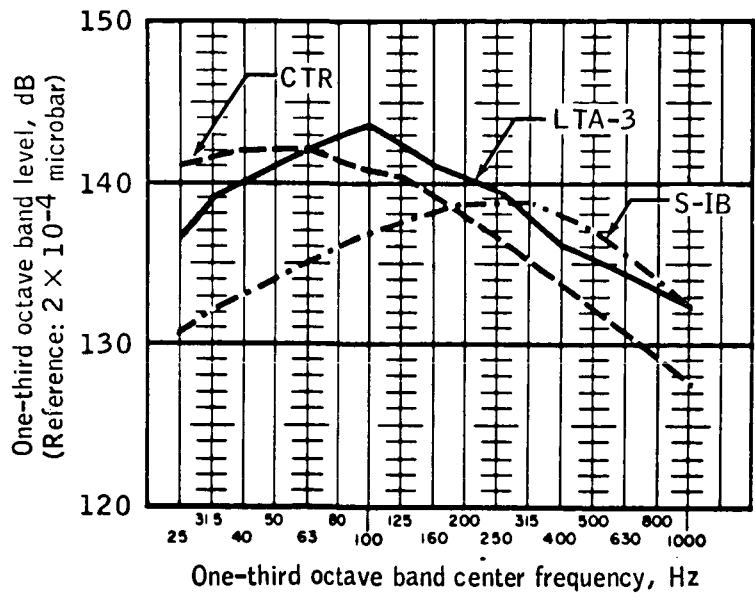


Figure 19. - Comparison of LTA-3 test and predicted spectra on SLA exterior.

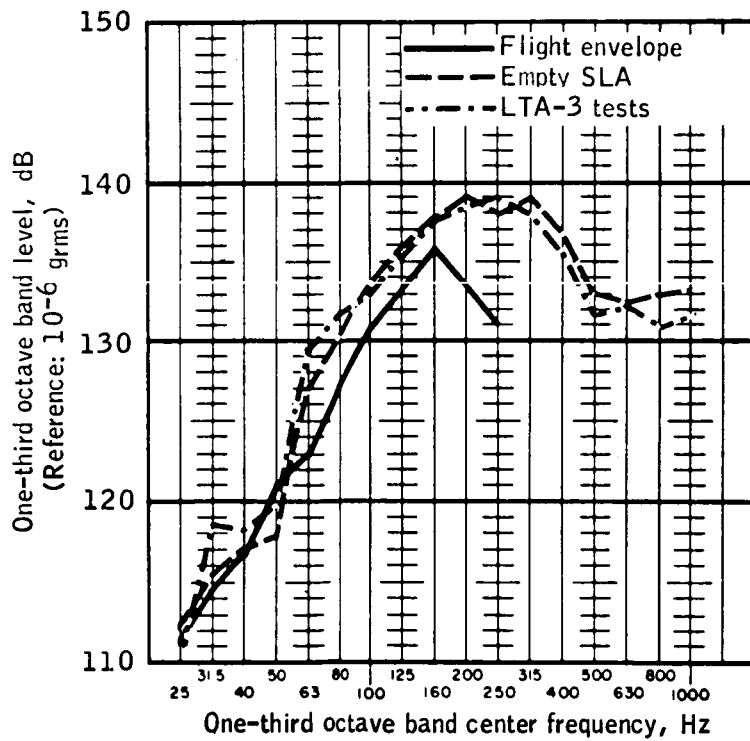


Figure 20. - Response spectrogram (SLA-0).

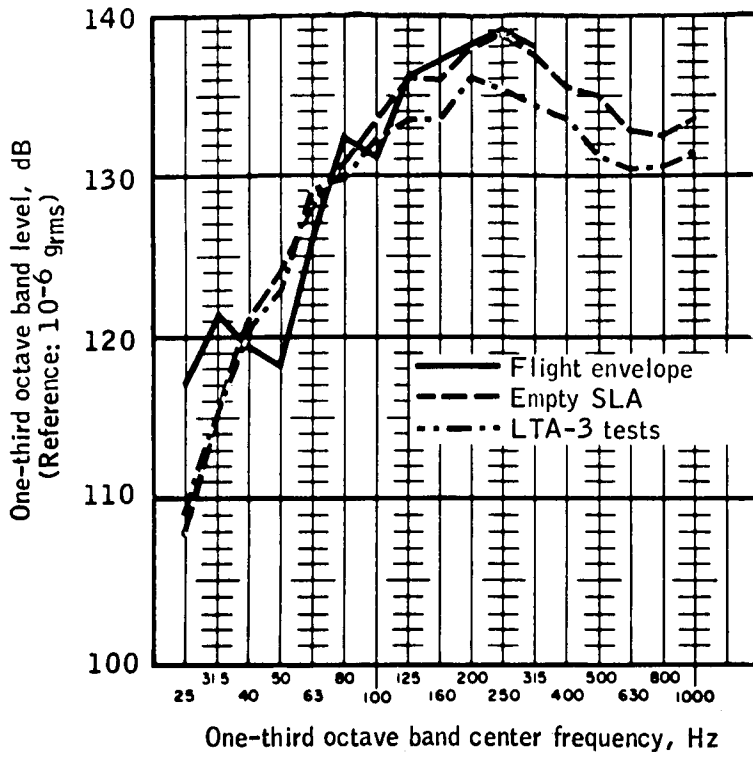


Figure 21. - Response spectrogram (SLA-1).

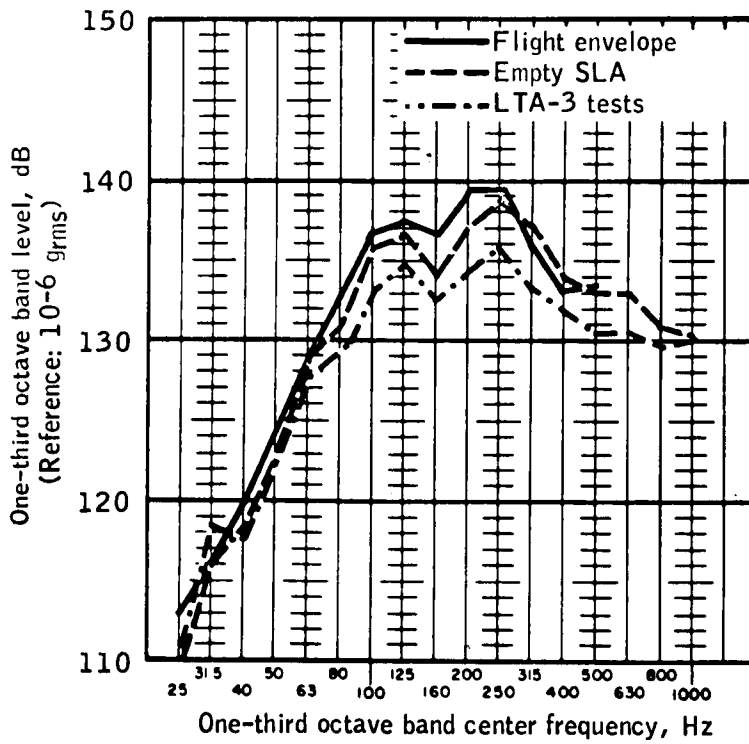


Figure 22. - Response spectrogram (SLA-2).